PNC TN9420 90-004

SUMMARY OF LMFBR SUBASSEMBLY BLOCKAGE STUDIES AT PNC

December, 1990

OARAI ENGINEERING CENTER

POWER REACTOR AND NUCLEAR FUEL DEVELOPMENT CORPORATION

〒319-1184　茨城県那珂郡東海村大字村松4番地49
核燃料サイクル開発機構
技術展開部　技術協力課

OFFICIAL USE ONLY
PNC TN9420 90-004
December, 1990

Summary of LMFBR Subassembly Blockage Studies at PNC

Hisashi Ninokata

Abstract

Experimental and analytical studies at PNC are reviewed on local flow blockage in simulated LMFBR wire-wrapped fuel subassemblies. Major aspects of the experimental investigations and correlations obtained are summarized. Partial blockage experiments were carried out on bundles of various sizes, e.g., 7-, 19-, 37-, 61- and 91-pin bundles with water as well as sodium as a working fluid. Water tests yielded fundamental data that were useful in building calculating models and in verifying the code. Sodium tests aimed at development of the practical correlations that were directly applied to evaluation of coolability of the Japanese Prototype FBR Monju driver core fuel subassemblies exposed to the partial blockage conditions. Some important correlations include those for the maximum temperature rise in recirculating flows behind the blockage in a given subassembly, the dryout condition, and the coolability of the bundles with a fission gas release into blockage wake region. A brief review of the analytical method is given. Some calculational results by the PNC subchannel code ASFRE are shown with respect to flow and temperature fields in partially blocked subassemblies.

Safety Engineering Division, Fast Breeder Reactor Safety Engineering Section
O-arai Engineering Center

社内一般
PNC TN9420 90-004
1990年12月

動燃における高速炉燃料集合体局所閉塞研究の概要

二ノ方　寿

要　旨

動燃における高速炉燃料集合体内局所閉塞研究は，主に少数本数のワイヤスペーサ型ピン束を用いた水流動試験及びナトリウム試験による実験的研究と，サブチャネル解析コードを用いた解析的研究に分けられて実施されてきた。

水を作動流体とする実験研究は，流動圧損特性や，コード検証に必要な流速及び温度分布データを提供した。ナトリウム実験では，局所閉塞を仮定した原型炉条件下での局所的冷却材温度上昇を評価する簡易手法の導出，ドライアウト迄の余裕や閉塞後流にFPガス放出があった場合の冷却性に対するモデルが開発された。これらの知見の概要を，本報告書に一括して示す。

解析的研究は，サブチャネル解析コードASFRE の開発・検証を中心として行われてきた。本報告書に，その開発・検証の現状と，ワイヤスペーサモデルの有効性に対する検証例として，厳密にワイヤスペーサ効果を考慮した場合と，等価な裸ピン体系で計算した場合の比較を述べる。

大洗工学センター　安全工学部　高速炉安全工学室

CONTENTS

List of Tables

List of Figures

1. INTRODUCTION

An assessment of the coolant thermohydraulic behaviors under local blockage conditions was required in connection with the local fault evaluation of the Japanese Prototype FBR Monju driver core fuel subassemblies. Major facets of the experimental investigations were directed toward the derivation of the empirical formula for estimating the flow reduction due to the blockage formation, temperature rise behind the blockage and, for local boiling, the transition of two-phase flow pattern and its effect on the critical heat flux condition in the actual wire-wrapped fuel pin subassemblies. Simultaneously efforts were also made in the area of computer code development to enhance quantitative representations of the phenomena. This paper is addressed to a review of these experimental and analytical efforts. Some important correlations described in this review include those for the maximum temperature rise in recirculating flows behind the blockage in a given subassembly, the dryout condition, and the coolability of the bundles with a fission gas release into blockage wake region. The last part of the review gives a summary of the computer code development and validation. Some calculational results by the PNC subchannel code ASFRE are shown with respect to flow and temperature fields in a partially blocked wire-wrapped pin subassembly.

2. PARTIAL BLOCKAGE WATER EXPERIMENTS[1,2]

(1) The tests using water as a working fluid were conducted with 61-bare rod bundles and wire-wrapped 61- and 169-pin bundles all with a central or wall blockage. Flow visualization indicated the recirculating flow is stable: without large oscillations discharging vortices out of the wake region. It was also found that the shape of recirculating flow regions for the wire-spacer pin bundles was almost identical with that for the blocked bare pin bundles.

This was considered to be due to the fact that the wake length (defined next) was shorter than the wire-wrap lead length.

(2) The wake length L_W, as defined by the distance between the blockage plane and the point where the flow changes its direction toward downward or reattachment point, was 1.7 - 1.8 times the characteristic length $d_B(= 2(A_B/\pi)^{0.5}$; A_B is the blocked area) of the central blockage and 2.7 - 3.0 times d_B of the wall blockage in the range of blockage Reynolds number $1.7 \times 10^4 \sim 3.4 \times 10^4$. It was shown that the dimensionless wake length depended on blockage Reynolds number Re_B and had approximately the same value for three blockages, i.e., 17 % and 38 % central and 50 % wall blockages:[1]

$$\frac{L_W}{d_B} = \frac{1}{0.723}(\log_{10} Re_B - 3.7). \quad (1)$$

The blockage Reynolds number Re_B was defined based on d_B and bundle mass flow rate.

(3) For these blocked bundles, velocity and static pressure distributions were obtained. The maximum reverse flow velocity amounted to about 70 % of the bundle average velocity. The mean velocity profiles in the mixing layer were common to all the tests and the width of the layer increased linearly with distance from the blockage. The trough of pressure behind the blockage almost coincided with the mixing layer.

(4) The dimensionless residence times τ^* ($= \tau U/d_B$; τ: fluid residence time, U: mean velocity in the unperturbed bundle) obtained by measurements of the decay of the concentration of injected salt in the wake region were independent of Reynolds number. τ^* were 10 for the 17 % central, 13 for the 17 % central and 26 for the 50 % wall blockage.

(5) Mass flow reductions due to the presence of partial blockage in subassemblies were measured with a constant pressure difference being applied between subassembly inlet and outlet. In addition to the wire-wrapped 61-pin bundles, the full scale wire-wrapped 169 pin bundles with five different central blockage sizes, i.e., 19 %, 42 %, 48 %, 59 % and 67 % and one wall blockage size of 41 % were used for the experiment. Form loss coefficients C_D of the blockages were reduced from the pressure drop and flow data. C_D were found to be

independent of bundle Reynolds number Re_B and were graphically represented as a function of the fraction of the blocked flow area as shown in Fig. 1. It was noted that the flow reduction was very small even for large blocked area fractions, e.g., 10 % reduction in flow against 60 % blockage.

(6) Distortion of the recirculating flow region behind the blockage due to leakage flows through a porous blockage was investigated. As the leakage flow rate increased, the recirculation zone diminished from its lower part and disappeared finally at the leakage flow ratio of 6 - 8 % to the total mass flow.

(7) Influences of gas release into the wake region on the flow field were investigated. Qualitatively, while a trend was observed that a local motion of the released gas was restricted by the wire-spacers nearby, a large bubble was also dispersed by the wire spacers and a bubbly flow regime prevailed in the downflow direction. Also it was observed that the continuously injected gas was transported by the wire-sweep flow of the liquid-phase and, as a result, was distributed through the downflow region of the whole bundle.

3. PARTIAL BLOCKAGE SODIUM EXPERIMENTS[3,4,5,6,7]

Several series of sodium tests were carried out from 1974 to 1982 using partially blocked wire-wrapped and grid-spacer pin bundles in the Sodium Boiling and Fuel Failure Propagation Test Facility, SIENA. All of the test series consisted of (i) single-phase flow tests, (ii) local boiling tests and (iii) simulated fission product (FP) gas release tests. In each of the test sections an impermeable blockage was formed by inserting a stainless steel plate in subchannels of a heater pin bundle. Table 1 summarizes the test section geometries, where the parameters are the number of pins, type of spacer (G: grid or W: wire), heated length, blockage category (C: central or E: wall), location of the blockage (a distance from the bottom

of the heated section toward the downstream direction) and blockage fraction. All the pins were 6.5 mm in diameter and arranged in a triangular array with pin pitch of 7.9 mm which are the representative of the Monju driver core fuel subassemblies.

Table 1 Summary of test sections

Test section	7GC	37GC	37WC	61WC	19GE	37GE	37WE	91WE
Pins	7	37	37	61	19	37	37	91
Heated length (mm)	450	456	455	450	460	459	455	300
heat flux distribution	uniform	←	←	←	←	←	←	←
Blockage type	C	C	C	C	E	E	E	E
Blockage location (mm)	350.5	304	300	255	300	308	255	20
Blockage area fraction (%)	44	39	26	36	58	58	50	50
Wire-wrap pitch (H) (mm)	-	-	265	265	-	-	265	265
Spacing of the grid spacers (mm)	200	200	-	-	200	200	-	-

3.1 Single-phase experiments

(1) Wake length L_W in the central blockage cases was expressed in terms of the blockage ring parameter N_R ($= D_B/P$; D_B is another definition of the characteristic length of the blockage and is given by Eq. (3); P is the pin pitch): [3,4]

$$\frac{L_W}{D_B} = 2.1\, N_R^{-0.1} \quad (\text{for } 2<N_R<12) \tag{2}$$

and

$$D_B = \sqrt{l_a \cdot l_W} \quad \text{for central blockage,} \tag{3}$$

l_a and l_W are defined in Fig. 2. Equation (2) was derived based on the PNC wire-wrapped 37- and 61-pin bundle experiments (sodium) and the KfK grid spacered 169-pin bundles (water) for various mass flow rates. It is seen from this expression that the wake length has little dependency on the spacer type. Equation (2) does not account for the Reynolds number effects; apparently the applicability of the model is restricted by the range of the data obtained in the experiments, i.e., for a high Reynolds number region.

(2) Based on the thermal and hydraulic balances between the sodium inside the wake region and the surrounding sodium flow with the heat exchange layer model, the following empirical formula for the coolant residence time was obtained for the central blockage cases:[4]

$$\frac{\tau U_B}{d_h} = 35.3\, N_R^{0.85} \tag{4}$$

and for the wall blockage cases:[6]

$$\frac{\tau U_B}{d_h} = 43.8\, N_R^{1.42} \tag{5}$$

where τ is the coolant residence time, U_B is the averaged flow velocity through the unblocked subchannels, d_h is the equivalent hydraulic diameter of the subchannels, N_R is the blockage ring parameter. D_B for the wall blockage is equal to l_a defined in Fig. 2.

(3) Figure 3 shows a typical two-dimensional isotherm map of the sodium temperature increase observed in a central-blocked wire wrapped 61-pin bundle experiment.[3] The empirical formula for estimating the maximum temperature in the wake, T_{max}, is given with the use of Eqs. (4) or (5):

$$T_{max} - T_B = C_B \cdot C_W \frac{\tau U_B}{d_h} \frac{4q''(1-F)}{c_p \rho U_0} \tag{6}$$

where T_B is the average sodium temperature outside the wake region. C_B and C_W are the bare rod bundle peaking factor(= 1.4 to 1.5), and the spacer wire distortion factor, C_W (= 1.2). These peaking factors were obtained by performing additional bare bundle blockage heat transfer experiments. q" is the heat flux, F is the fraction of the blocked flow area, c_p is the specific heat of sodium, ρ is the sodium density and U_0 is the inlet flow velocity.

(4) A typical result of applying Eq. (6) to an operating conditions of Monju is illustrated in Fig. 4, from which it is seen that the central-type blockage will not cause local boiling unless the flow reduction is extremely large. However, for the wall blockage cases, the estimated temperature rises are much higher than the central blockage cases: even the medium sized wall blockage of about 25 % could result in onset of local boiling under the operating conditions of Monju.

3.2 Boiling experiments[3,5,6]

(1) Local boiling tests were performed on the test sections 7GC, 37GE, 37WC, 37WE and 61WC (Table 1). Both stable and unstable boiling modes were observed depending on the operating conditions: i.e., the unstable mode was dominating under low-heat-flux and low-flow conditions and/or under the low inlet subcooling condition. So was the stable mode under high flow and high inlet subcooling conditions. In general the stable mode had less margin to dryout.

(2) The wall blockage experiments were of more interests than the central blockage cases as has been explained in 3.1.(4). Critical heat flux data including KfK 169 pin bundle data were correlated with the boiling inception heat flux q''_{IB} for various bundle flow velocities as shown in Fig. 5. The shaded zones represent the stable boiling regions. From the concept of the convection controlled heat transfer, the straight lines were drawn so that the all data of KfK were fitted by linear relations between each combination of q''_{cr}, q''_{IB}, and U_B, while one boiling inception data of the PNC bundle configuration was shown based on Eq. (6). q''_{cr} and q''_{IB} are the critical heat flux and the boiling inception heat flux.

(3) In Fig. 5, q''_{cr} data of KfK fell on lines as expressed by:[6]

$$q''_{cr} = \begin{bmatrix} 1.38 \\ 1.56 \\ 1.61 \end{bmatrix} q''_{IB}, \quad \text{for } \Delta T_{sub} = \begin{bmatrix} 510 \\ 430 \\ 350 \end{bmatrix} \tag{7}$$

Here ΔT_{sub} is the inlet subcooling. The linear relations among q''_{cr}, q''_{IB}, and U_B suggest that the dryout condition of stable boiling could be predicted by an extension of the single-phase flow concept. That is, the excess temperature in the absence of the boiling, ΔT_{ms}, was evaluated by the following equation:[7,8]

$$\Delta T_{ms} = \Delta T_{sub} \frac{(q''/U_B)_{cr} - (q''/U_B)_{IB}}{(q''/U_B)_{IB}} . \tag{8}$$

ΔT_{ms} for the KfK 169-pin 21% blocked bundle was nearly constant (= 208±20°C) at the instance of permanent dryout and ΔT_{ms} for the PNC 37-pin 50% blocked bundle was 74°C.

The difference between KfK and PNC ΔT_{ms} values was considered as being caused by the difference in subchannel flow areas.[6]

3.3 Effects of FP gas release behind blockage[9]

To investigate the combined thermohydraulic effects of local blockage and fission products (FP) gas release, gas release tests were performed using 37GC, 37GE, 37WC, 37WE and 61WC test sections. Figure 6 shows typical data of a transient gas release test where a severe temperature rise behind the blockage is shown.[9] Figure 7 summarizes the effects of gas release rate on the temperature rise behind the blockage, where the temperature rise is normalized by:

$$\Theta = \frac{d_h}{4} c_p (T-T_B) \frac{U_B}{q''} \quad . \tag{9}$$

Except for the 37GC case (Case 2), the temperature rise primarily depends on the gas release rate and is independent of the type of spacers, blockage location and gas injection point.

4. ANALYTICAL STUDIES ON PARTIAL BLOCKAGES

4.1 Computer code development [10,11]

Two series of efforts on single-phase subchannel analysis code development have been made: UZU and ASFRE. While the UZU code was developed for the specific purpose of the partial blockage analysis and calculated the steady-state thermal hydraulics,[10] the ASFRE code series aimed at both steady-state and transient calculations with and without the partial flow blockage in a subassembly.[11] In the following, a brief description of ASFRE is given.

(1) ASFRE-I for grid-spacered and ASFRE-II for wire-wrapped pin subassemblies were developed in 1970s and had been used extensively for the experimental analysis of the PNC 37-pin bundle experiments, evaluation of the partial blockage in Monju subassemblies for

licensing purposes and the 9th and 10th LMBWG Benchmark Exercises on partial blockages in KfK bundles.[12,13] The numerical scheme used in these subchannel codes was based on the fractional time step method and the modified MAC method. However, because of the explicit treatment of many terms in conservation equations, time step sizes required to run the code stably were very small and hence the total CPU cost usually was enormously high. The wire spacer model in ASFRE-II was of the crossflow forcing function type which assumed the transverse mass flow rate due to the wire forced flow component. This model is solely based on mass continuity considerations and does not account for the momentum conservation. Nevertheless it was a good approximation of the wire effects for highly turbulent and forced convection flows.

(2) ASFRE-III was developed in order to eliminate those drawbacks in ASFRE-I and -II. The crossflow forcing function model was replaced by the distributed resistance model (DRM)[14] which accounted for the wire spacer effects by additional resistance terms in both axial and lateral momentum equations. As a result, the code is applicable to forced and mixed convection problems and local and inlet completed blockage problems in wire-wrapped pin subassemblies. The numerical scheme is based on the modified ICE technique: three governing equations (mass, momentum and energy) are reduced to a set of Newton-Raphson iteration equations and solved simultaneously. Because the energy equation is coupled with the other equations, the method is suitable to solve mixed to natural convection flow problems where a strong coupling of velocity and temperature field is important.

4.2 Some examples of flow blockage simulations by ASFRE

(1) ASFRE-III was applied to the 37-pin bundle sodium experiment 37WL-200-6 with the test section 37WC. Major experimental conditions of the experiment were: inlet flow velocity is 3.59 m/s; average heat flux is 56.83 w/cm^2; and inlet flow temperature is 261.2°C.

In order to see effects of wire-spacers on the flow and temperature fields, two calculations were carried out: Case 1 with full wire spacer model (DRM) and Case 2 without wire spacer model. Case 2 is a calculation for the bare rod bundle equivalent to the wire wrapped bundle; equivalent in the sense that geometrical parameters such as flow areas and equivalent hydraulic diameters were adjusted on an average basis for the presence of the wire-wraps. Figures 8 and 9 displays the predicted flow and temperature distributions of Case 1(DRM) and Case 2. Figure 8 clearly indicated the "distorted" or "twisted" fields caused by the wire-wrapping in contrast to the Case 2 result given in Fig. 9. In general, agreement of the predicted sodium temperatures by the DRM were fairly good: the maximum temperature rise just behind the blockage plane is 84.9°C in the experiment and 91.4°C in the prediction; whereas the Case 2 (bare rod approximation) predicted 79.2°C. The higher temperature prediction for the wire-wrapped bundle was due to a local wire-wrap effect: i.e., local crossflow was blocked by the wire spacer located periodically at the pin-to-pin gap and the local stagnation of the flow caused a higher temperature rise. The predicted wire spacer distortion factor C_W is, then, 1.15 which is close to 1.2 obtained experimentally.

(2) ASFRE-I was applied to the 9-th LMBWG Benchmark Exercises (169-pin central blockage problems)[12] and 10-th LMBWG Benchmark Exercises (169-pin wall blockage problems).[13] The calculated results were in good agreement with the experiments. Figure 10 shows a typical result by ASFRE for the LMBWG Benchmark Problem: 21 % permeable corner blockage.

(3) The shape of recirculation zone is significantly affected by the blockage edge configuration as were shown in experiments. These facts in the experiments were well simulated by ASFRE as shown in Fig. 8 and Fig. 10. The KfK bundle had the blockage at the grid spacer position and the grid spacer worked as a flow regulator which directed the flow. As a result, the wake region was prolonged toward the downstream direction. Whereas in the PNC bundle experiments, it was clearly observed that the main flow which passed the

blockage side was pulled toward the wake region which made the recirculating region rather short. As a result, the hottest spot was localized near the blockage plate in the PNC bundles.

5. SUMMARY

Firstly, the experimental studies of partial flow blockage using water as a working fluid have been reviewed. Flow visualization and measurement of the flow and temperature distributions as well as the static pressure distribution yielded fundamental data for the wire-wrapped pin bundles that were useful in building calculational models and verifying the subchannel analysis codes.

Secondly, the sodium flow partial blockage experiments have been reviewed with a summary of the correlations which were practical in an evaluation of the coolability of Monju driver core fuel subassemblies exposed to the partial blockage conditions. They include correlations for the maximum temperature rise in the wake region behind the blockage, margins to the fuel pin dryout, and the coolability of the subassemblies with a fission gas release into the blockage wake region.

Finally, a brief review of the computer code development and application has been given. Typical examples of the calculational results by a PNC subchannel code ASFRE have been shown: one for the PNC wire-wrapped 37-pin central blockage sodium experiment and one for the KfK grid spacered 169-pin bundle (with a 1/2 symmetry) experiment with a permeable wall blockage.

The wire spacer effects on the flow and temperature fields were, in general, localized. A global shape of the recirculating wake regions was almost the same as the wake shape produced in the equivalent bare rod bundle with the blockage. However as a result of local thermohydraulic interactions of fluid with the wire spacers, the temperature and velocity fields

were "twisted" and a hottest spot in the recirculation region gave about 10 - 20 % higher fluid temperature than that of equivalent bare rod bundle configurations.

Acknowledgement

The author acknowledges that this review was made possible owing to helpful suggestions and many PNC internal reports as well as open publications provided by Dr. K. Haga and Mr. H. Nakamura of O-arai Engineering Center, PNC.

References.

1. H. Nakamura, et al., "Hydraulic experiment on local blockage of fuel subassembly (1); Flow reduction and flow visualization tests," Proc. 1976 Fall Mtg. Atomic Energy Society of Japan, B68, Tokai, Japan, October 1976.

2. H. Nakamura, et al., "Hydraulic simulation of local blockage in a LMFBR fuel subassembly," Nucl. Eng. Des., 62 (1980) 323 - 333.

3. K. Haga, et al., "Review and future needs of experimental studies on local faults," Proc. BNES Conf. on the Science and Technology of Fast Reactor Safety, Guernsey, U.K., May 1986.

4. K. Yamaguchi, et al., "Experimental investigation of local cooling disturbances in LMFBR fuel subassemblies," Proc. 1981 ASME Winter Meeting, Washington D.C., USA, 81-WA/HT-40, 1981.

5. M. Uotani, et al., "Experimental investigation of sodium boiling in partially blocked fuel subassemblies," Nucl. Eng. Des., 82 (1984) 319-328.

6. K. Yamaguchi, et al., "Boiling and dryout conditions in distributed cluster geometry and their application to the liquid-metal fast breeder reactor local fault assessment," Nucl. Sci. Eng., 88 (1984) 464-474.

7. A.J. Clare, "Pin cooling and dryout in steady local boiling," KfK-2944, April 1980.

8. B. Dorr and J.E.De Vries, "The ECN/KfK local boiling experiments in Petten," Proc. 8th LMBWG Meeting, Mol, October 1978.

9. K. Haga, et al., "Experimental study on the effect of fission product gas release into blockage wake region using a simulated LMFBR fuel subassembly," Nucl. Eng. Des., 82 (1984) 329-340.

10. K. Miyaguchi, "Analytical studies on local flow blockages in LMFBR subassemblies using the UZU code," Nucl. Eng. Des., 62 (1980) 25-38.

11. H. Ninokata, et al., "ASFRE-III: A computer program for triangular rod array thermohydraulic analysis of fast breeder reactors," PNC N941 85-106, July 1985.

12. J. Ishimaru, et al., "A verification study of the ASFRE code through experimental analysis to local flow blockage tests," Proc. the 9th LMBWG Meeting, Casaccia, Italy, June 1980.

13. H. Ninokata, et al., "The application of ASFRE to the 10th LMBWG Benchmark Tests," Proc. 10th LMBWG Meeting, Karlsruhe, FRG, October 1982.

14. H. Ninokata, et al., "Distributed resistance modeling of wire-wrapped rod bundles," Nucl. Eng. Des., 104 (1987) 93-102.

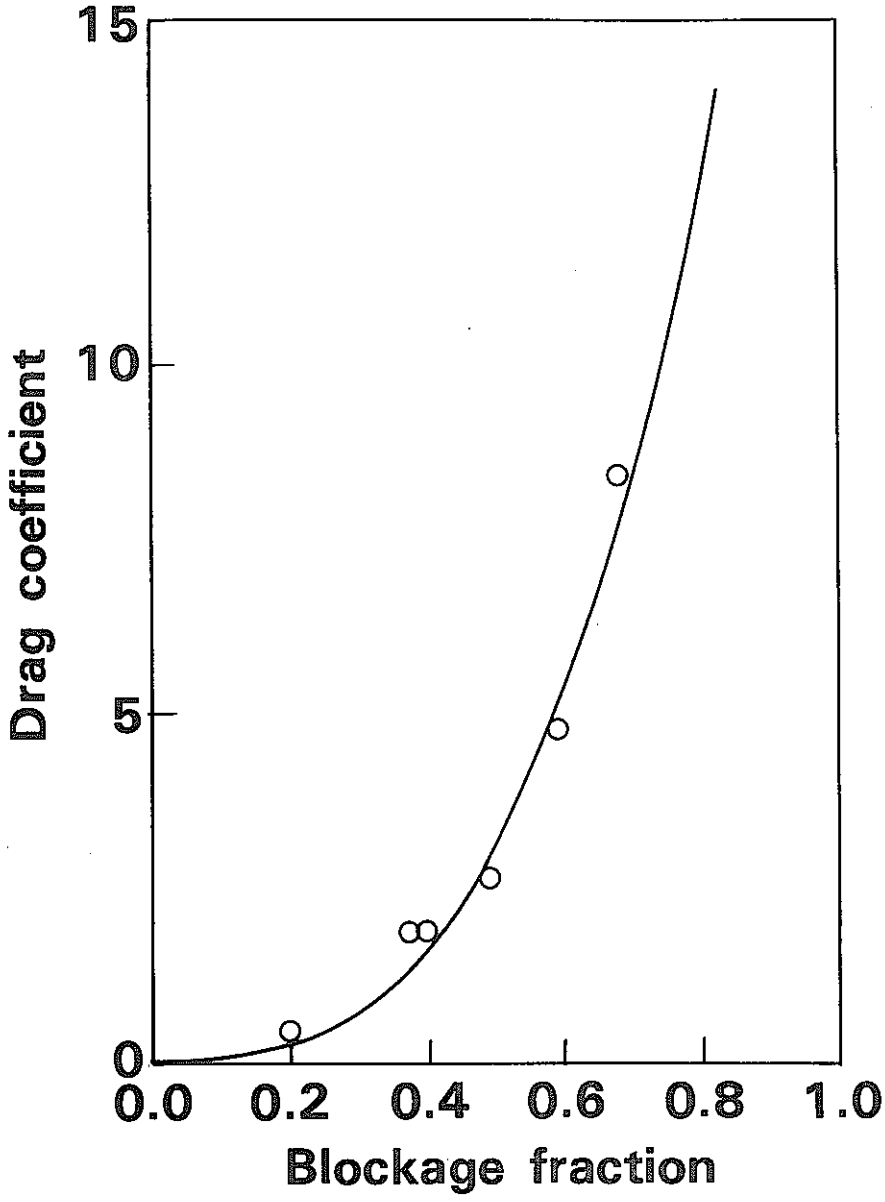

Fig.1 Correlation for drag coefficient of blockage with blockage fraction

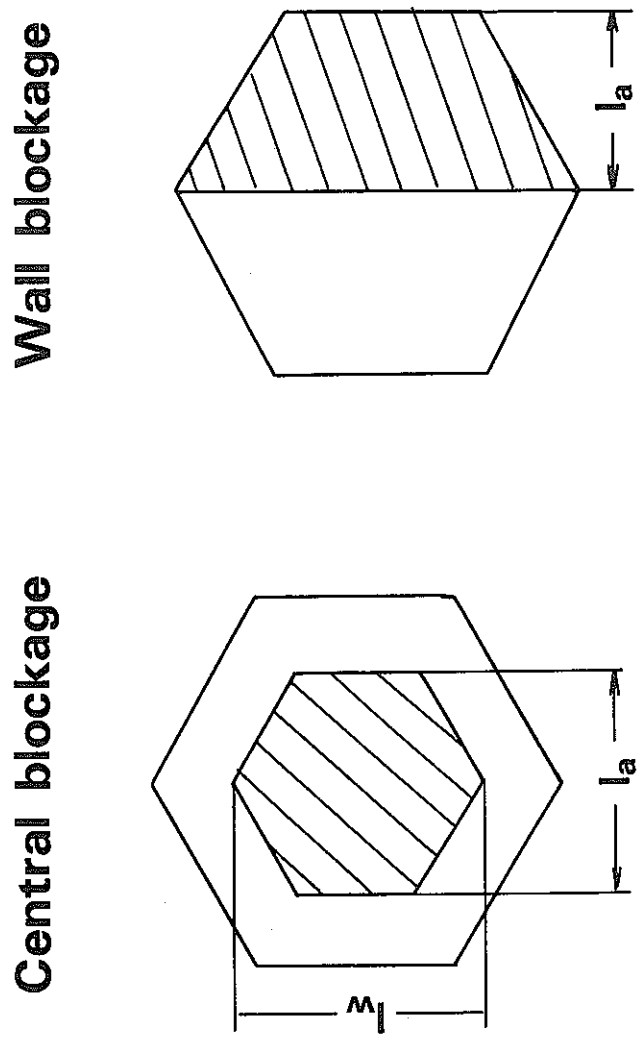

Fig.2 Definition of l_a and l_w of blockages

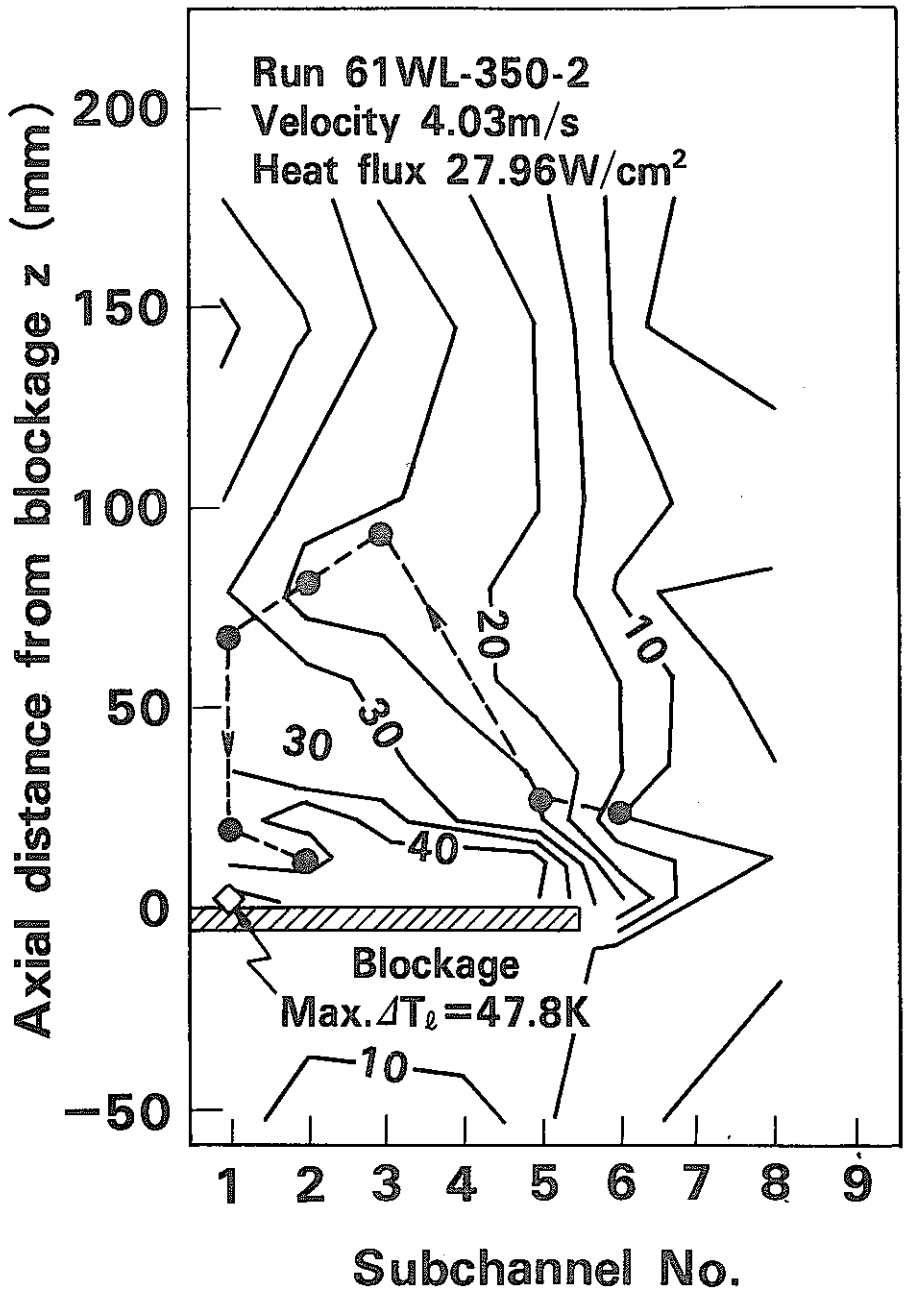

Fig.3 Typical isotherms of sodium behind the blockage of 61-pin bundle test section

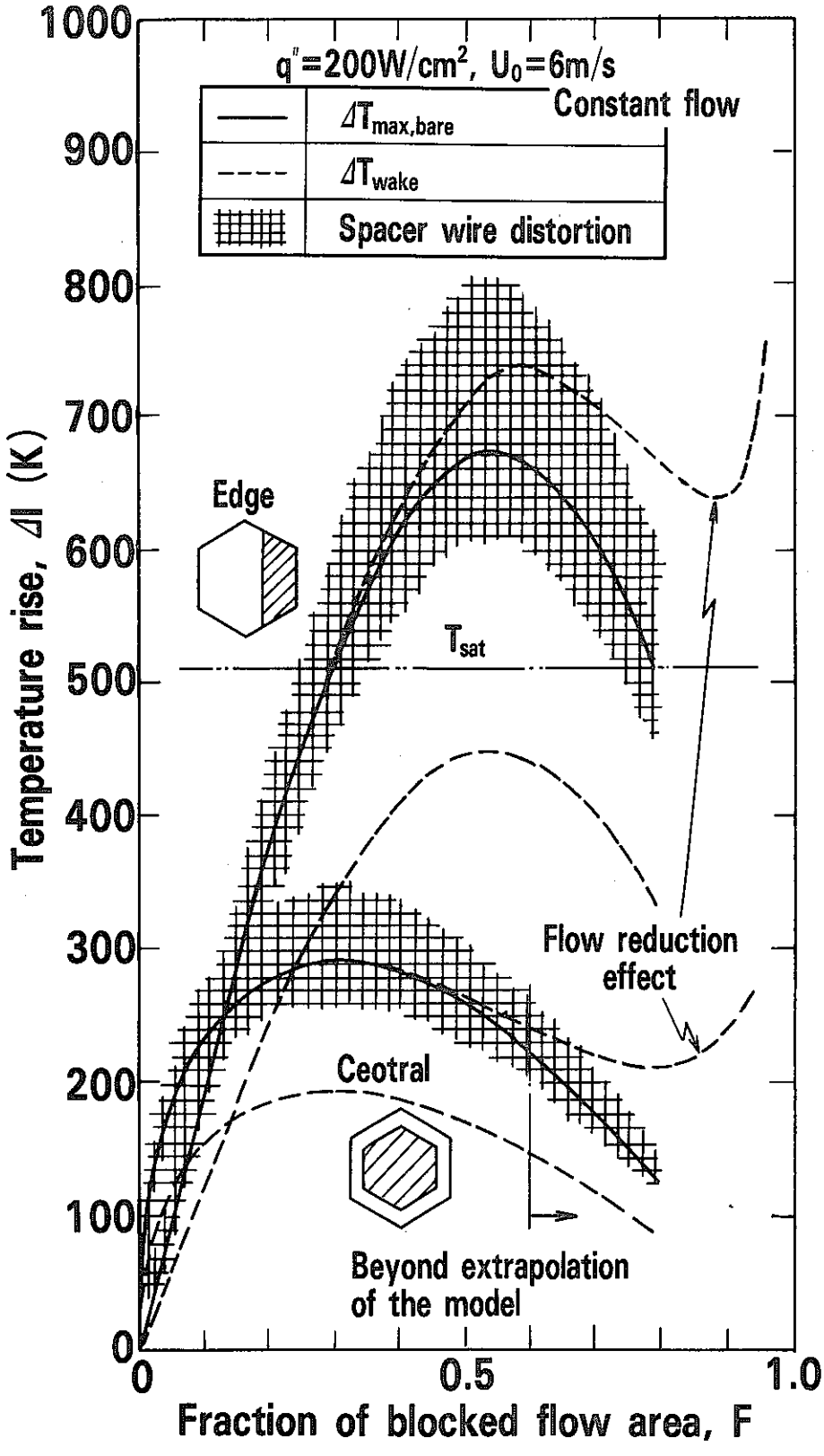

Fig.4 Estimation of temperature rise under a Monju operating condition (single-phase calculation)

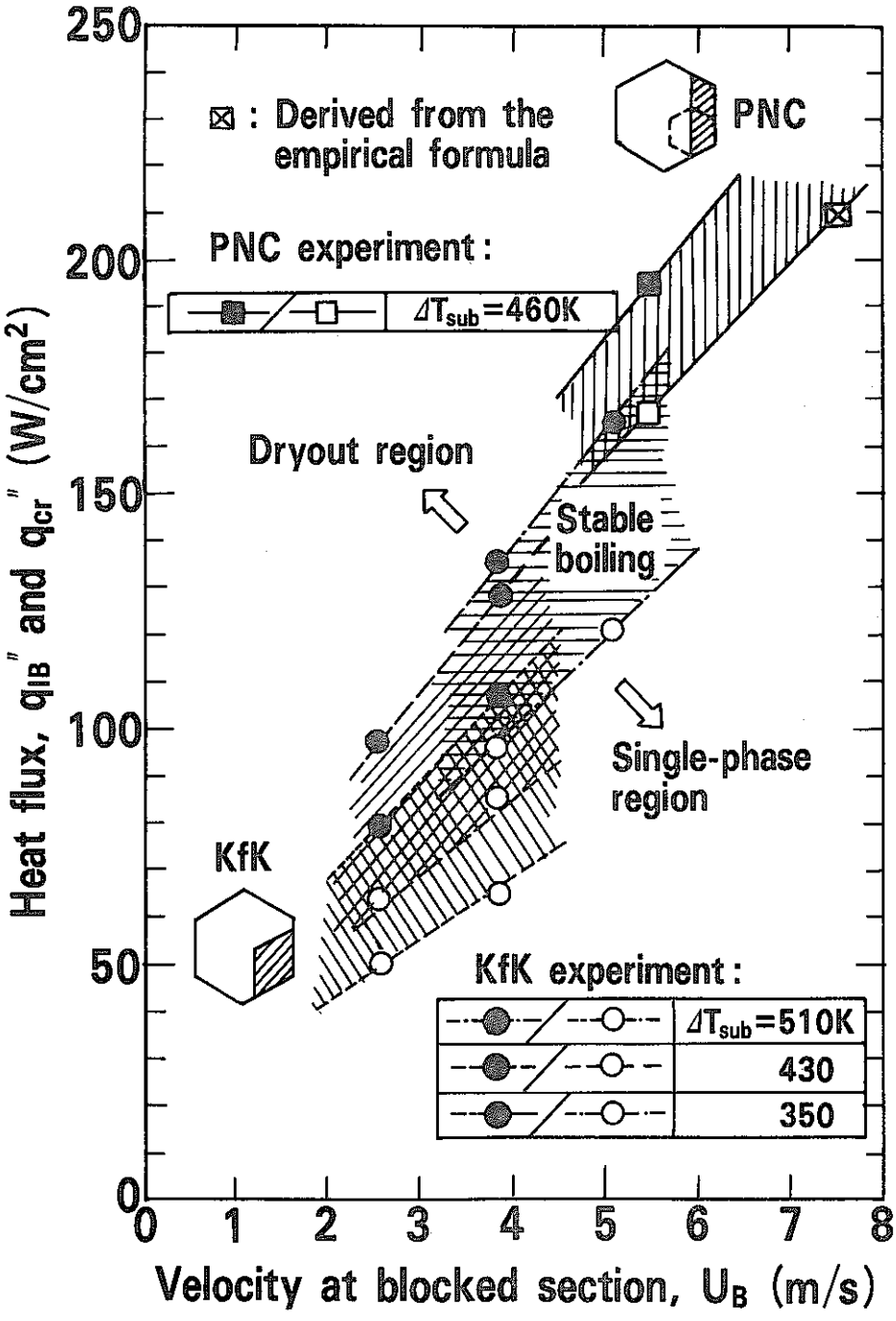

Fig.5 Correlations of the boiling inception and dryout in cases of ~20% wall and corner blockages

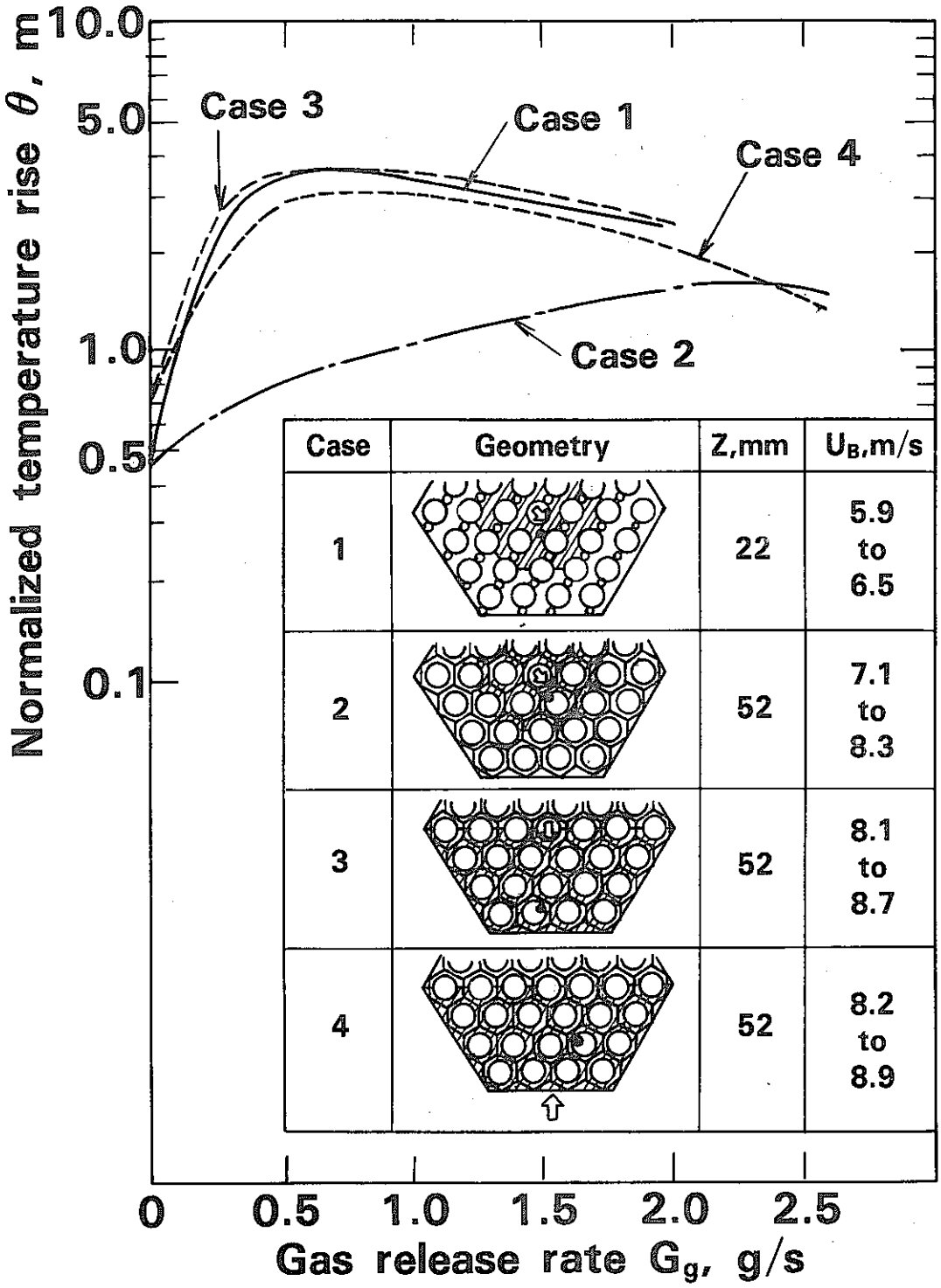

Fig.6 Effect of gas release rate on temperature rise in wake region under various geometrical conditions

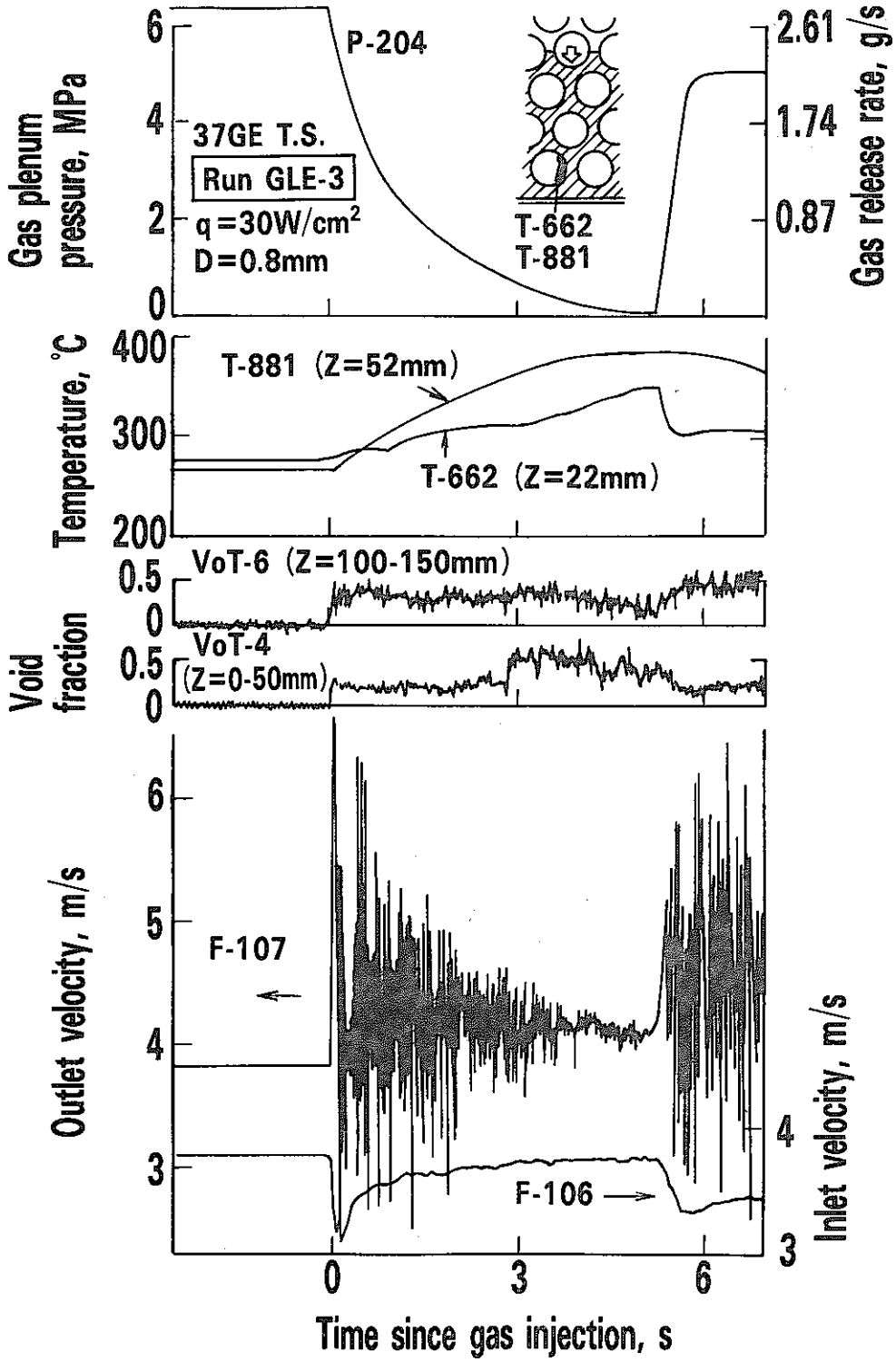

Fig.7 Dynamic behaviors of gas plenum pressure, temperature, void fraction and coolant velocity measured in transient gas injection test ; Run GLE-3

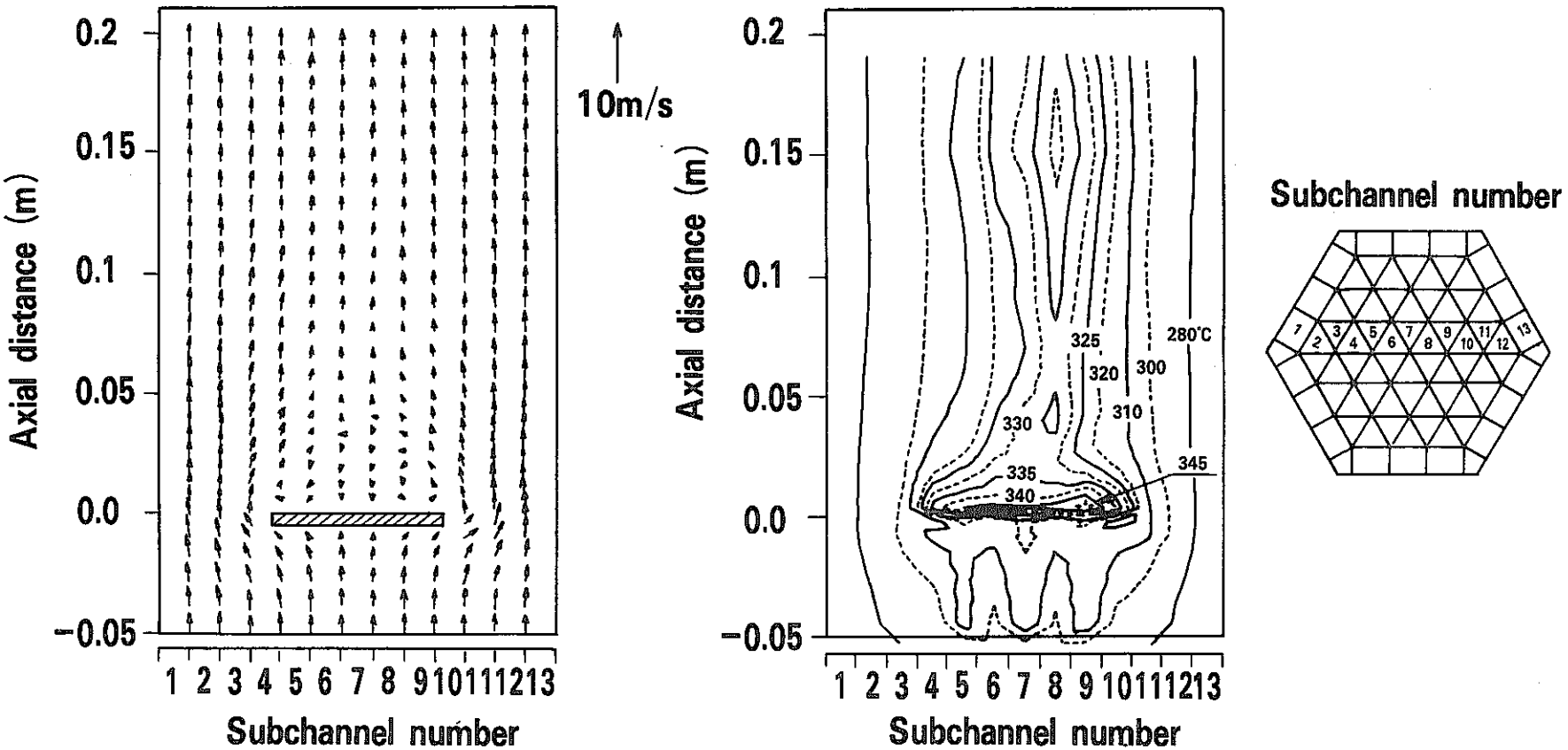

Fig.8 Flow velocity and temperature distributions for the wire-wrapped pin bundle with a central blockage predicted by the ASFRE-III code (Case 1)

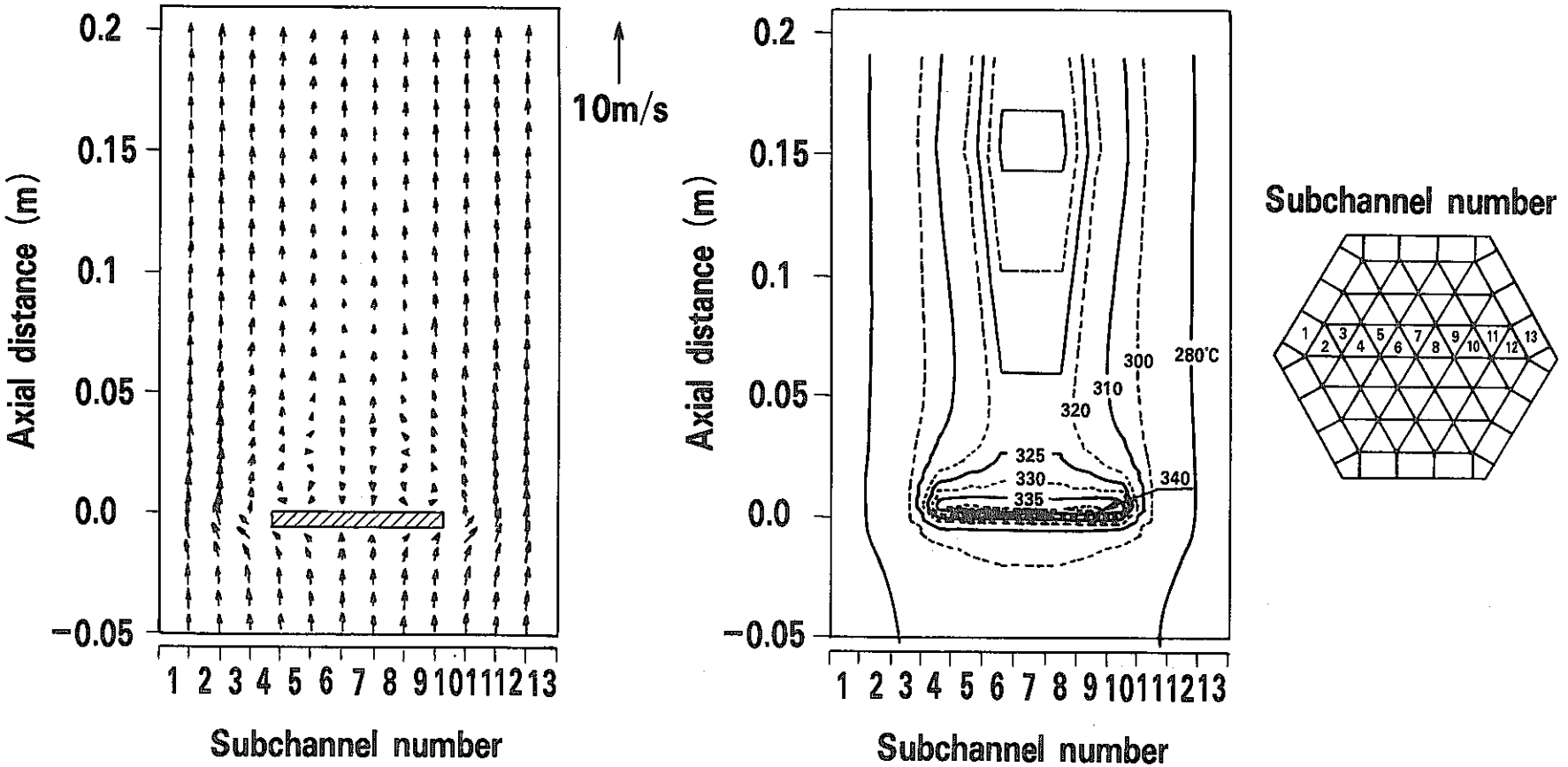

Fig.9 Flow velocity and temperature distributions for the equivalent bare pin bundle with a central blockage predicted by the ASFRE-III code (Case 2)

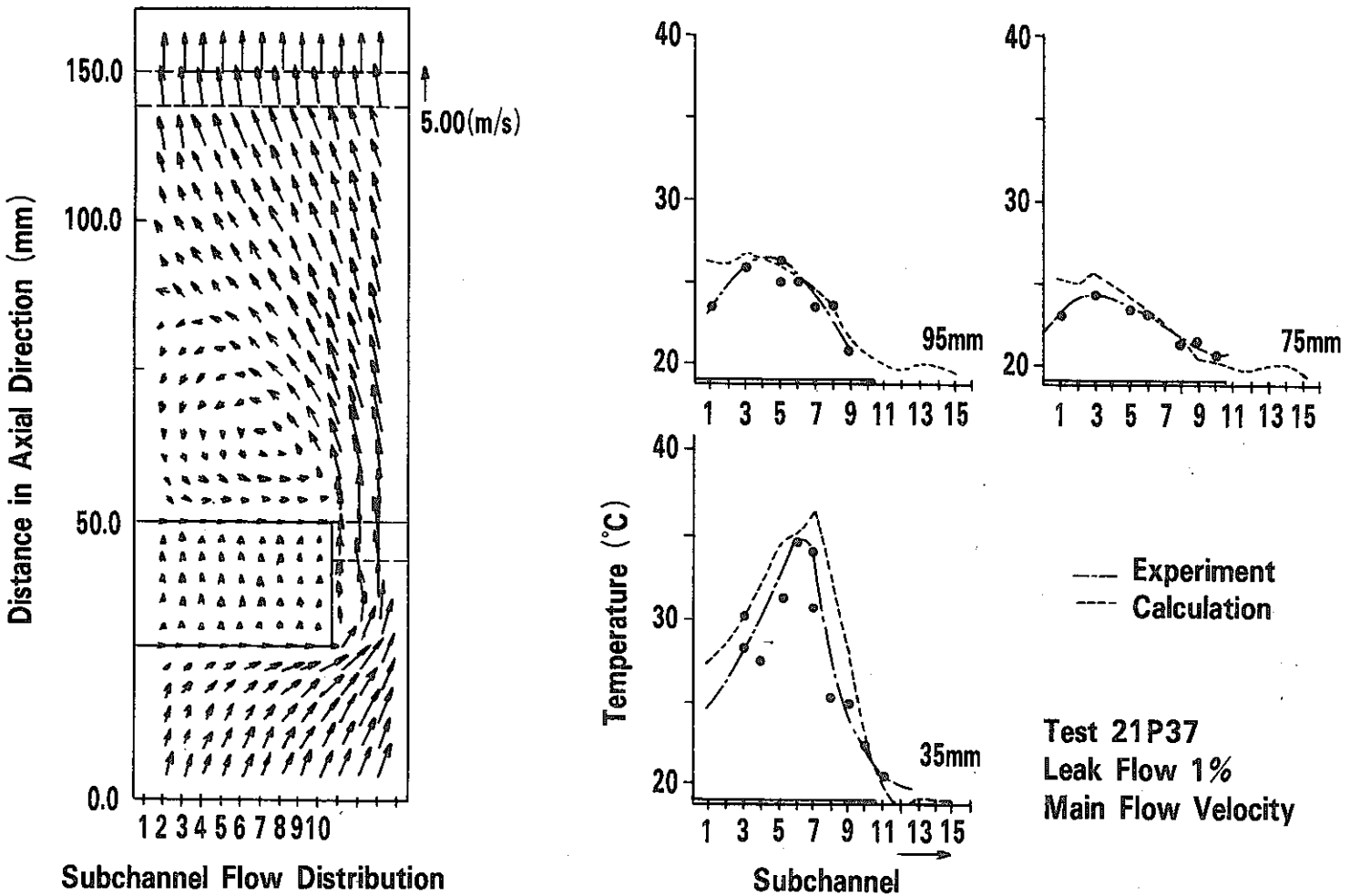

Fig.10 Calculational example by ASFRE-I for the 10th LMBWG Benchmark Problem: 21% permeable corner blockage